Biological Psychiatry

Priority Communication

Dopaminergic Regulation of Nucleus Accumbens Cholinergic Interneurons Demarcates Susceptibility to Cocaine Addiction

Joo Han Lee, Efrain A. Ribeiro, Jeongseop Kim, Bumjin Ko, Hope Kronman, Yun Ha Jeong, Jong Kyoung Kim, Patricia H. Janak, Eric J. Nestler, Ja Wook Koo, and Joung-Hun Kim

ABSTRACT

BACKGROUND: Cholinergic interneurons (ChINs) in the nucleus accumbens (NAc) play critical roles in processing information related to reward. However, the contribution of ChINs to the emergence of addiction-like behaviors and its underlying molecular mechanisms remain elusive.

METHODS: We employed cocaine self-administration to identify two mouse subpopulations: susceptible and resilient to cocaine seeking. We compared the subpopulations for physiological responses with single-unit recording of NAc ChINs, and for gene expression levels with RNA sequencing of ChINs sorted using fluorescence-activated cell sorting. To provide evidence for a causal relationship, we manipulated the expression level of dopamine D_2 receptor (DRD2) in ChINs in a cell type–specific manner. Using optogenetic activation combined with a double whole-cell recording, the effect of ChIN-specific DRD2 manipulation on each synaptic input was assessed in NAc medium spiny neurons in a pathway-specific manner.

RESULTS: Susceptible mice showed higher levels of nosepoke responses under a progressive ratio schedule, and impairment in extinction and punishment procedures. DRD2 was highly abundant in the NAc ChINs of susceptible mice. Elevated abundance of DRD2 in NAc ChINs was sufficient and necessary to express high cocaine motivation, putatively through reduction of ChIN activity during cocaine exposure. DRD2 overexpression in ChINs mimicked cocaine-induced effects on the dendritic spine density and the ratios of excitatory inputs between two distinct medium spiny neuron cell types, while DRD2 depletion precluded cocaine-induced synaptic plasticity.

CONCLUSIONS: These findings provide a molecular mechanism for dopaminergic control of NAc ChINs that can control the susceptibility to cocaine-seeking behavior.

https://doi.org/10.1016/j.biopsych.2020.05.003

Drug addiction is a neuropsychiatric disorder characterized by compulsive and persistent drug seeking along with excessive motivation to consume substances. Epidemiologic studies revealed that only a small subset of the population exposed to cocaine develops addiction-related symptoms (1,2). Owing to the socioeconomic burdens of cocaine addiction, the behavioral and neurobiological changes after exposure to cocaine have been extensively studied in rodent models for the past several decades. However, the molecular profile of drug addiction and the cellular mechanism underlying susceptibility to cocaine addiction remain largely unresolved, in part owing to the lack of reliable mouse models demonstrating individual differences.

The mesolimbic dopaminergic (DAergic) pathway, which includes the nucleus accumbens (NAc), is dysregulated in various states of drug addiction (3). The NAc predominately comprises medium spiny neurons (MSNs), which are divided into two subtypes based on expression of different DA receptor subtypes: DA D_1 receptor MSNs (D1-MSNs) and DA D_2 receptor MSNs (D2-MSNs). They produce two functionally distinct outputs of the NAc: D1-MSNs mainly form the direct pathway that promotes reward-related behaviors, while D2-MSNs form the indirect pathway that serves a critical role in aversion and negative reinforcement (4,5). In the NAc, both types of MSNs receive excitatory inputs from the basolateral amygdala (BLA), ventral hippocampus (vHPC), and medial prefrontal cortex (mPFC). All inputs are capable of inducing reinforcement (6), but each pathway is independently regulated after withdrawal from cocaine self-administration (7). However, the functional distinctions and regulatory mechanisms of these pathways for cocaine seeking remain elusive.

MSNs can be regulated by several types of striatal interneurons (8,9). A growing body of evidence suggests that cholinergic interneurons (ChINs) in the NAc might play critical roles in processing reward- and addiction-related information (10,11). Despite comprising a minute portion (1%–2%) of the entire NAc neuronal population, ChIN axonal fields are widespread (12), leading to extensive modulation of a large number of NAc neurons including MSNs. In fact, cocaine exposure induces both ChIN activation and acetylcholine (ACh) release (13), and ablation of NAc ChINs results in an exaggerated

SEE COMMENTARY ON PAGE 738

 ISSN: 0006-3223

locomotor response to noncontingent cocaine injections (14). Consistently, locomotor sensitization is prevented by an increase in NAc ACh levels (15). NAc ChINs also receive direct inputs from mesolimbic DAergic neurons, which activate ChINs primarily through glutamate co-release (16). Once activated by the firing of DAergic neurons, NAc ChIN firing is paused, which is in part mediated by activation of the DA D_2 receptor (DRD2) (17). Conversely, selective activation of NAc ChINs causes DA release through activation of nicotinic ACh receptors (nAChRs) expressed on the axonal terminals of DAergic neurons (18). Given these anatomical and physiological observations, modification of NAc ChINs would potentially control neuronal features and synaptic plasticity of MSNs, which could consequently contribute to addiction-like behaviors.

Here, we employed a behavioral paradigm to quantify motivation for cocaine after extended self-administration in mice, which allowed for a segregation of subject animals exhibiting susceptibility versus resilience to cocaine-seeking behaviors. We also conducted RNA sequencing on isolated ChINs from the NAc of susceptible and resilient mice to obtain differential gene expression at the whole transcriptome level, which indicated that the downstream DRD2 signaling pathway was upregulated in susceptible animals. To examine the cellular mechanism and functional impact on cocaine seeking, we exploited cell type–specific manipulation of DRD2 and then monitored physiological and behavioral changes. Taken together, our findings indicate that DRD2 abundance in NAc ChINs is both necessary and sufficient for development of susceptibility to cocaine seeking, which is mediated by a pathway-specific modulation of structural and synaptic plasticity in distinct MSN subtypes.

METHODS AND MATERIALS

For detailed methods, see the Methods and Materials in Supplement 1. Briefly, wild-type male mice were subjected to cocaine self-administration (1.2 mg/kg/infusion), which was conducted for 23 hours/day. After 10 daily progressive ratio (PR) sessions, the subject mice were divided into susceptible or resilient groups based on the average breakpoint of the last 3 days. The breakpoint was defined as the number of active nosepoke responding to receive the last infusion. Subsets of mice identified as susceptible or resilient were then subjected to an extinction or punishment procedure. During 7-day extinction (1 hour/day), nosepoke responding resulted in no consequence. Using distinct subsets of mice, the baseline level of nosepoke response was assessed for 3 days with a fixed ratio 5 schedule without any presentation of punishment. For subsequent 3 days, electric foot-shocks were randomly presented as a punishment, by one-third chance upon each active nosepoke. Other subsets of susceptible and resilient mice were employed for in vivo extracellular recording, RNA sequencing of sorted ChINs, ex vivo slice recordings, or single-cell reverse transcriptase polymerase chain reaction experiment.

For cell type–specific manipulations, we used adult male Chat-Cre or Chat-Cre/Drd2-eGFP double transgenic mice. We bilaterally injected an adeno-associated virus (AAV) into the NAc, which allowed for Cre-specific DRD2 overexpression, DRD2 knockdown, or expression of DREADD (designer receptor exclusively activated by a designer drug) derived from the kappa opioid receptor (KORD) (19). For optogenetic experiments, a channelrhodopsin-2 (ChR2)–expressing AAV was additionally injected into the mPFC, vHPC, or BLA. After injection, at least a 5-week recovery period was allowed prior to ex vivo patch clamp recordings, morphological analysis, or behavioral assessments. To assess postsynaptic current in DRD2 knockdown mice, cocaine-HCl (15 mg/kg) was intraperitoneally injected for 5 consecutive days, followed by 1-day withdrawal.

RESULTS

Segregation of Susceptible and Resilient Mice by Behavioral Phenotypes

We sought to divide inbred C57BL/6 mice based on the level of motivation toward the contingent consumption of cocaine. To accomplish this, we devised a behavioral paradigm modified from a self-administration procedure previously used for a rapid increase in drug motivation in rats (20). The procedure consists of a fixed ratio 1 schedule for cocaine infusion followed by a 10-day PR schedule (Figure 1A). The final breakpoints, which were measured as an index of motivation, were distributed over a wide range, with a local minimum around breakpoint 32 (Figure 1B). We employed a k-means clustering analysis using final breakpoints and time-out responding (Figure S1A in Supplement 1) to systematically separate a mouse population into high- and low-motivation groups (division at breakpoints at 32.33) (Figure 1B). As expected, mice displaying high motivation showed progressively increasing levels of responding toward cocaine infusions throughout the 10-day assessment, which was significantly higher than the low-motivation group (Figure 1C and Figure S1B–E in Supplement 1). Interestingly, the difference in cocaine intake between groups was undetectable during the initial acquisition (Figure S1F in Supplement 1), and the initial acquisition efficacy (as measured by the latency to accomplish 40 infusions) was not predictive of the final measures of motivation (Figure S1G in Supplement 1).

Consistent with our hypothesis that the motivation index could represent susceptibility to addiction-related phenotypes, mice with high motivation exhibited other core addiction-like behaviors. Compared with the low-motivation animals, the high-motivation group exhibited higher levels of nosepokes during random presentation of electric foot-shocks at the time of each active nosepoke (Figure 1D and Figure S1H, I in Supplement 1), which indicates drug seeking despite receiving contingent punishment. Mice in the high-motivation group also displayed a higher level of seeking behaviors during the extinction procedure, as they performed more nosepokes than low-motivation mice in the absence of cocaine infusion (Figure 1E). Finally, mice in the high-motivation group exhibited more impulsive seeking behaviors than mice in the low-motivation group, as assessed by the number of nosepokes during a postinfusion time-out period (Figure S1J, K in Supplement 1) (21). Collectively, these behavioral analyses supported our notion that the high- and low-motivation groups represented animals that were susceptible and resilient, respectively, to express addiction-like behaviors.

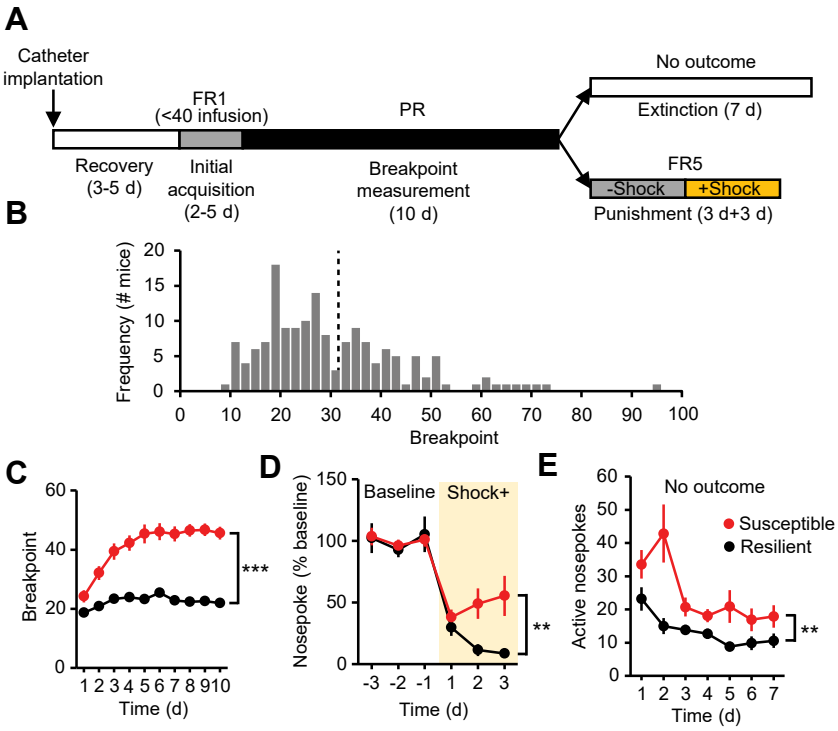

Figure 1. Segregation of mouse populations based on susceptibility to addiction-like behaviors after cocaine self-administration. **(A)** A timeline of experimental procedure. After initial acquisition and breakpoint measurement using cocaine self-administration, a subset of mice were subjected to an extinction or punishment procedure. **(B)** A summary histogram showing final breakpoints that individual mice displayed. The dotted line depicts the borderline breakpoint that divides susceptible and resilient animals. **(C)** Daily breakpoints that resilient (n = 102 mice) and susceptible (n = 56 mice) groups displayed throughout PR sessions (group × time [$F_{9,495}$ = 9.12, $p < .001$]). **(D)** Relative numbers of active nosepokes despite random delivery of electric foot-shocks (group × time [$F_{5,40}$ = 4.11, $p < .01$]; susceptible: n = 10 mice; resilient: n = 7 mice). **(E)** Number of active nosepokes under cocaine unavailability (group × time [$F_{6,72}$ = 3.51, $p < .01$]; susceptible: n = 11 mice; resilient: n = 13 mice). **(C–E)** Two-way repeated-measures analysis of variance was used. $^{**}p < .01$, $^{***}p < .001$. Data are presented as mean ± SEM. FR, fixed ratio; PR, progressive ratio.

Activation of NAc ChINs by Cocaine Infusion Is Blunted in Susceptible Mice

We recorded NAc ChINs to examine whether and how ChINs of susceptible and resilient mice responded differently to systemic cocaine infusion. After catheter implantation and cocaine self-administration, single-unit recording was conducted from the NAc shell region in vivo (Figure 2A, B and Figure S2A, B in Supplement 1). The unit activity of putative ChINs was identified by interspike interval and spike frequency (10). Consistent with previous reports (13,22), intravenous infusion of cocaine increased ChIN firing rates in drug-naïve control mice (Figure 2C). We also observed elevated ChIN activity in the resilient group (Figure 2D) but failed to detect any significant alterations of ChIN activity of the susceptible mice (Figure 2E). Hence, NAc ChIN activity would be affected in susceptible mice where it could potentially play instructive roles for progressive ratio responding.

Higher *Drd2* Expression in NAc ChINs of Susceptible Mice

Neural and behavioral plasticity underlying drug addiction are associated with altered expression of numerous genes in the NAc (23). To capture those changes on a transcriptome-wide level, we exploited fluorescence-activated cell sorting to perform cell type–specific RNA sequencing from NAc ChINs after completion of the PR schedule (Figure 3A; Figure S3A, B in Supplement 1; and Table S1 in Supplement 1). As expected, sorted ChINs expressed a significantly higher level of *Chat*, a molecular marker for ChINs, and contained only marginal levels of messenger RNAs (mRNAs) encoding marker proteins for other striatal interneuron subtypes and MSNs (Figure 3B). Differential expression analysis (fold change > 2 and false discovery rate < .01) identified 2909 differentially expressed genes (DEGs) in NAc ChINs from susceptible mice compared with resilient mice. These DEGs were composed of 1685 upregulated genes and 1224 downregulated genes (Figure 3C, D and Table S2 in Supplement 2). Our DEG analysis also revealed that the most abundant readouts were transcripts of protein-coding genes (66.8%), followed by long noncoding RNAs (12.9%) and pseudogenes (8.3%), with the remaining categories accounting for 12.1% (Figure S3C in Supplement 1), similar to those of NAc D1- and D2-MSNs (24). However, there was little overlap of responsive DEGs (only 11 DEGs in common) between SST (somatostatin)-positive interneurons and NAc ChINs (Figure S3D in Supplement 1) (25).

KEGG (Kyoto Encyclopedia of Genes and Genomes) pathway analysis of upregulated DEGs in NAc ChINs from susceptible mice revealed that DAergic signaling was one of the top three upregulated pathways in susceptible animals (Figure 3E and Table S3 in Supplement 2). Other highly affected pathways, including long-term potentiation, endocytosis, and cAMP/cGMP (cyclic adenosine monophosphate/cyclic guanosine monophosphate) signaling, are also implicated in DAergic signaling (26,27). Gene Ontology terms related to DAergic signaling, such as cytoskeleton organization and small GTPase-mediated signaling, were identified (Figure 3F) (28,29). Among genes involved in DAergic signaling, upregulation of *Drd2* was of particular interest, as DRD2s in ChINs are proposed to regulate neuronal activity,

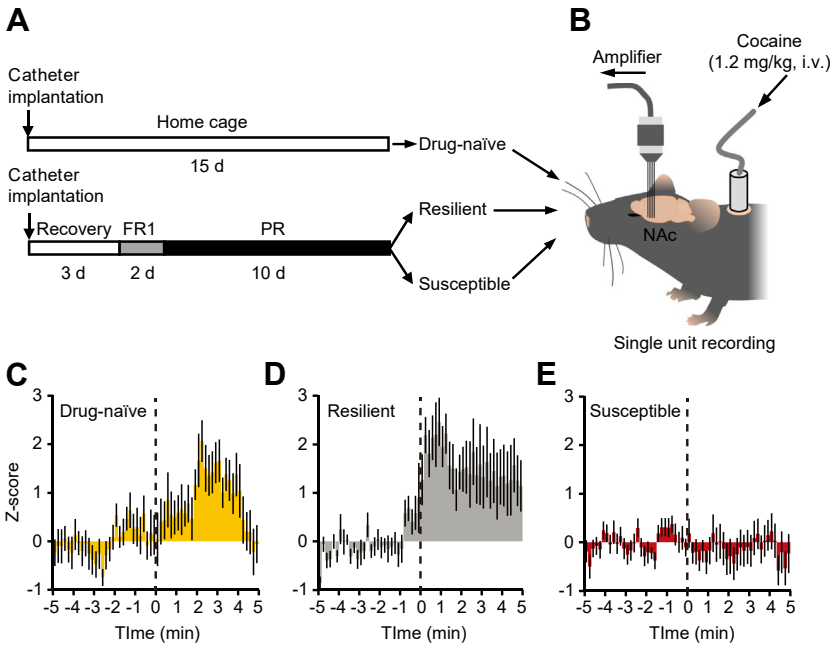

Figure 2. In vivo single-unit recording from the NAc cholinergic interneurons in each group of mice. **(A)** An experimental timeline for identifying resilient/susceptible mice. Drug-naïve mice were implanted with an i.v. catheter and kept in the home cage until recording. Recordings were conducted from resilient and susceptible mice after 3-day withdrawal from the last PR test. **(B)** A schematic illustration of in vivo single-unit recording. Cocaine (1.2 mg/kg, i.v.) was injected through a catheter connected to the right jugular vein during recording. **(C)** The average firing rate of putative cholinergic interneuron units in drug-naïve mice during the first exposure to cocaine (1.2 mg/kg, i.v.) is presented as a *z* score (n = 9 units from 5 mice). Unit recordings from **(D)** resilient (n = 12 units from 8 mice) or **(E)** susceptible (n = 23 units from 9 mice) mice. Recordings were conducted after 3-day withdrawal from the final PR test. Dotted lines indicate the onset of i.v. cocaine injection. Data are presented as mean ± SEM. FR, fixed ratio; i.v., intravenous; NAc, nucleus accumbens; PR, progressive ratio.

synaptic plasticity, and behaviors (30,31). Also, increased DRD2 activity, owing to its elevated abundance in ChINs of susceptible mice, could potentially counteract the cocaine-triggered activation of ChINs observed in control and resilient mice (Figure 2C).

One of physiological consequences that higher expression of DRD2 in ChINs can produce would be exaggerated DRD2-mediated reduction of neuronal activity (30). We perfused a DRD2 agonist quinpirole onto acute brain slices containing the NAc and measured spontaneous firing rates of NAc ChINs in a cell-attached configuration (Figure 4A–C). Quinpirole successfully decreased spontaneous activity of NAc ChINs (Figure 4D). The quinpirole-induced inhibition of ChIN activity was intact under treatment with a cocktail of synaptic blockers (APV, DNQX, and picrotoxin), suggesting that the DRD2-mediated reduction of neuronal activity was independent of synaptic inputs (Figure S4A in Supplement 1). To elucidate the possible correlation between drug motivation and DRD2 abundance in NAc ChINs, we assessed the final breakpoints from the PR test and the magnitude of DRD2-mediated inhibition by performing ex vivo cell-attached recordings (Figure 4A). Importantly, the magnitude of firing rate reduction by quinpirole positively correlated with measured breakpoints (Figure 4E). Furthermore, dispersed levels of DRD2 abundance appeared not to arise from an innately conferred difference, given that magnitudes of firing rate reduction were more widely distributed after completing the PR test, compared with drug-naïve control animals (Figure S4B, C in Supplement 1). We also measured *Drd2* mRNA levels by quantitative reverse transcriptase polymerase chain reaction with aspirated intracellular contents of ChINs from mice subjected to cocaine self-administration (Figure 4A, F and Figure S4D in Supplement 1). Indeed, single-cell quantitative reverse transcriptase polymerase chain reaction corroborated higher levels of *Drd2* mRNAs in NAc ChINs of susceptible mice than in those of resilient mice (Figure 4G).

DRD2 in NAc ChINs Is Sufficient and Necessary for Cocaine Seeking

To examine whether increased abundance of DRD2 was sufficient to induce addiction-like behavior, we overexpressed DRD2 by microinjecting Cre-dependent AAV vectors into the NAc of Chat-Cre mice. We confirmed the selective overexpression by co-labeling of turboGFP (turbo green fluorescent protein) and ChAT (choline acetyltransferase) (Figure S5A–D in Supplement 1), and validated that firing rates were further reduced by quinpirole in DRD2-overexpressing ChINs compared with uninfected control ChINs without affecting the baseline firing rate (Figure 5A and Figure S5E in Supplement 1). Importantly, Chat-Cre mice with DRD2 overexpression in NAc ChINs exhibited higher motivation toward cocaine infusion than Cre-negative control animals (Figure 5B–E and Figure S5F, G in Supplement 1). The increased motivation was unlikely due to reduced anxiety-like behavior, as novelty-induced suppression of feeding was comparable between the two groups (Figure S5H in Supplement 1).

To determine whether DRD2 in NAc ChINs was required for development of addiction-like behaviors, we next depleted DRD2 in NAc ChINs using a Cre-dependent knockdown AAV (32). We microinjected Cre-dependent knockdown AAV expressing a short hairpin RNA against the *Drd2* (shDrd2) into the NAc of Chat-Cre mice (Figure 5F) and confirmed that most of the ChAT-positive neurons expressed eYFP (enhanced yellow fluorescent protein), which was coexpressed in cells expressing shDrd2 (Figure S5I–L in Supplement 1) (32). Using cell-attached recordings, we validated that DRD2 knockdown

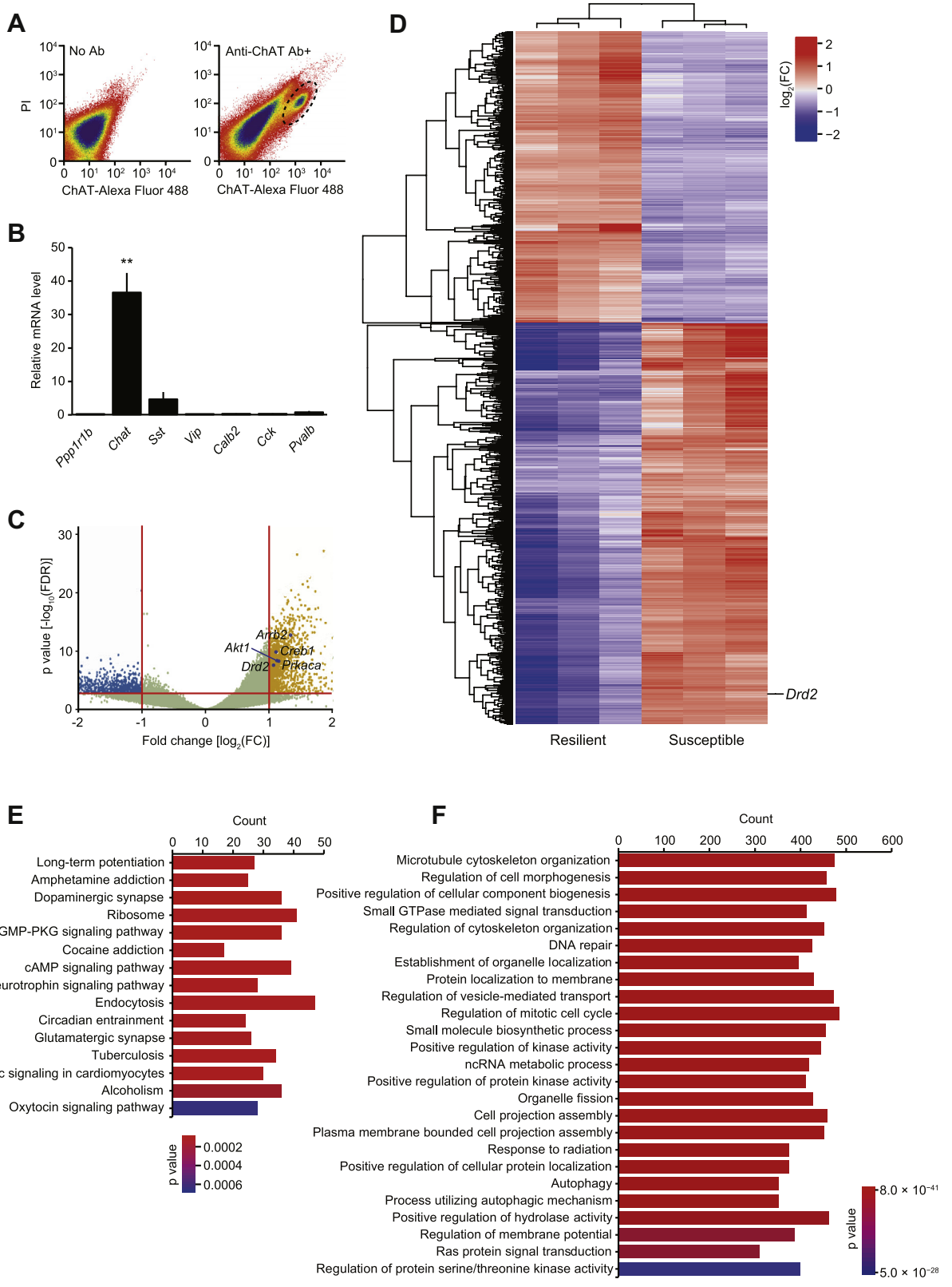
A
No Ab
Anti-ChAT Ab+
PI
ChAT-Alexa Fluor 488
B
Relative mRNA level
**
Ppp1r1b
Chat
Sst
Vip
Calb2
Cck
Pvalb
C
p value [-log10(FDR)]
Fold change [log2(FC)]
Arrb2
Akt1
Creb1
Drd2
Prkaca
D
log2(FC)
Drd2
Resilient
Susceptible
E
Count
Long-term potentiation
Amphetamine addiction
Dopaminergic synapse
Ribosome
cGMP-PKG signaling pathway
Cocaine addiction
cAMP signaling pathway
Neurotrophin signaling pathway
Endocytosis
Circadian entrainment
Glutamatergic synapse
Tuberculosis
Adrenergic signaling in cardiomyocytes
Alcoholism
Oxytocin signaling pathway
p value
F
Count
Microtubule cytoskeleton organization
Regulation of cell morphogenesis
Positive regulation of cellular component biogenesis
Small GTPase mediated signal transduction
Regulation of cytoskeleton organization
DNA repair
Establishment of organelle localization
Protein localization to membrane
Regulation of vesicle-mediated transport
Regulation of mitotic cell cycle
Small molecule biosynthetic process
Positive regulation of kinase activity
ncRNA metabolic process
Positive regulation of protein kinase activity
Organelle fission
Cell projection assembly
Plasma membrane bounded cell projection assembly
Response to radiation
Positive regulation of cellular protein localization
Autophagy
Process utilizing autophagic mechanism
Positive regulation of hydrolase activity
Regulation of membrane potential
Ras protein signal transduction
Regulation of protein serine/threonine kinase activity
p value

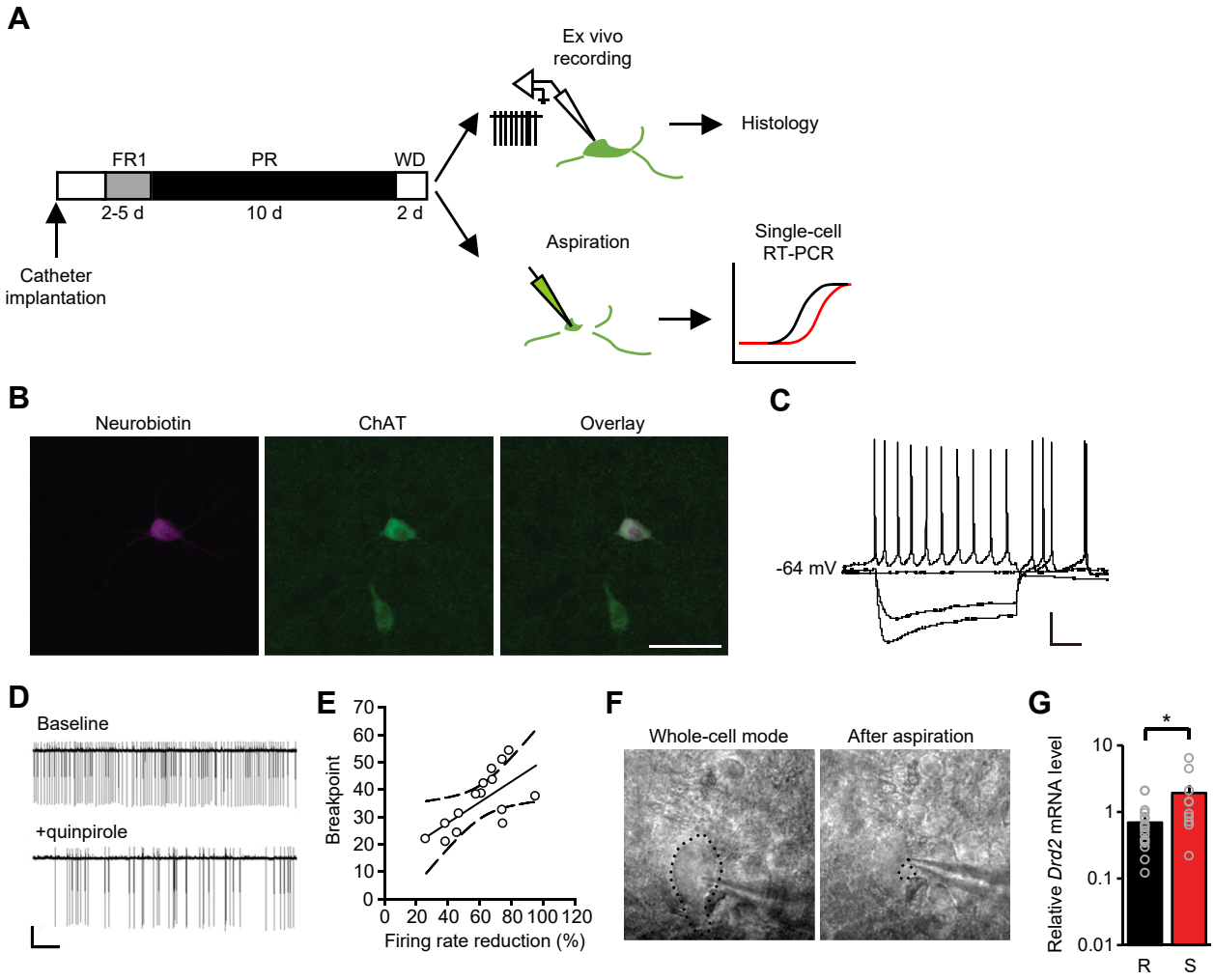

Figure 4. Elevated DRD2 abundance in NAc ChINs of susceptible mice. **(A)** Schematic workflow of measuring DRD2 abundance and testing physiological change in NAc ChINs between resilient and susceptible mice. **(B)** Confocal images of an example recorded NAc ChIN. Neurons were recorded with cell-attached recording, and neurobiotin was injected during subsequent whole-cell recording. Recorded cells were verified by co-labeling of neurobiotin (purple) and ChAT (green). Scale bar = 50 μm. **(C)** Representative traces of whole-cell recording in NAc ChINs. One-second current steps (−200, −100, 0, and +50 mV) were applied. Note that the recording was performed after bath application of quinpirole during cell-attached recording. Scale bars = 20 mV and 200 ms. **(D)** Representative traces of a cell-attached recording in NAc ChINs before (baseline) and after (+quinpirole) bath application of quinpirole (1 μM). Scale bars = 20 pA and 6 seconds. **(E)** Correlation between the level of motivation toward cocaine infusion and magnitude of firing rate reduction by quinpirole application (Pearson's correlation coefficient, $r = .668$, $p < .01$, $n = 15$ mice). Dotted lines represent the 99% confidence interval. **(F)** DIC images of a putative ChINs in acute brain slices before (whole-cell mode) and after aspiration of intracellular contents. Dotted lines delineate the ChIN soma, which is initially selected by its large soma size. **(G)** Relative amounts of *Drd2* mRNA in ChINs of resilient ($n = 18$ cells from 4 mice) and susceptible ($n = 10$ cells from 4 mice) groups (Mann-Whitney *U* test, $^*p < .05$). Data are presented as mean ± SEM. ChAT, choline acetyltransferase; ChINs, cholinergic interneurons; DIC, differential interference contrast; DRD2, dopamine D_2 receptor; FR, fixed ratio; mRNA, messenger RNA; NAc, nucleus accumbens; PR, progressive ratio; R, resilient; RT-PCR, reverse transcriptase polymerase chain reaction; S, susceptible; WD, withdrawal.

Figure 3. Cell type–specific RNA sequencing of susceptible and resilient mice shows upregulated DRD2 signaling in NAc ChINs of susceptible mice. **(A)** Representative fluorescence-activated cell sorting gating for isolation of NAc ChINs. Isolated and suspended NAc cells from wild-type mice were incubated with or without an Alexa Fluor 488-conjugated antibody against ChAT. **(B)** Expression levels of various neuronal markers in sorted ChAT+ cells, as assessed by reverse transcriptase polymerase chain reaction ($n = 4–5$ experiments). *Chat* transcripts were highly enriched in the Ab+ fraction. *Ppp1r1b* (DARPP-32) as a marker for medium spiny neurons and markers for individual GABAergic interneurons such as *Sst*, *Vip*, *Calb2*, *Cck*, and *Pvalb* were assessed (Student's paired *t* test [$t_3 = 6.02$, $p < .01$], relative to mRNA levels of individual genes in No Ab fraction). Data are presented as mean ± SEM. **(C)** Volcano plot based on *p* values and FCs of individual genes highlights differentially expressed genes in NAc ChINs of susceptible mice ($n = 9$ mice). Example genes implicated in the dopamine signaling pathway are specified. **(D)** Heatmap illustration for differentially expressed genes in ChINs of susceptible mice, with a red-to-blue gradient depicting upregulation (red) and downregulation (blue). Each row represents an individual experiment ($n = 3$ mice per experiment). **(E)** KEGG pathway analysis indicating responsive signaling pathways in NAc ChINs of the susceptible group compared with the resilient group. **(F)** Gene Ontology enrichment analysis of differentially expressed genes showing the altered expression of genes that are intimately involved in dopaminergic signaling, such as cytoskeleton organization and small GTPase-mediated signaling. $^{**}p < .01$. Ab, antibody; cAMP, cyclic adenosine monophosphate; cGMP, cyclic guanosine monophosphate; ChAT, choline acetyltransferase; ChINs, cholinergic interneurons; DRD2, dopamine D_2 receptor; FC, fold change; FDR, false discovery rate; GABAergic, gamma-aminobutyric acidergic; KEGG, Kyoto Encyclopedia of Genes and Genomes; mRNA, messenger RNA; NAc, nucleus accumbens; ncRNA, noncoding RNA; PI, propidium iodide; PKG, protein kinase G.

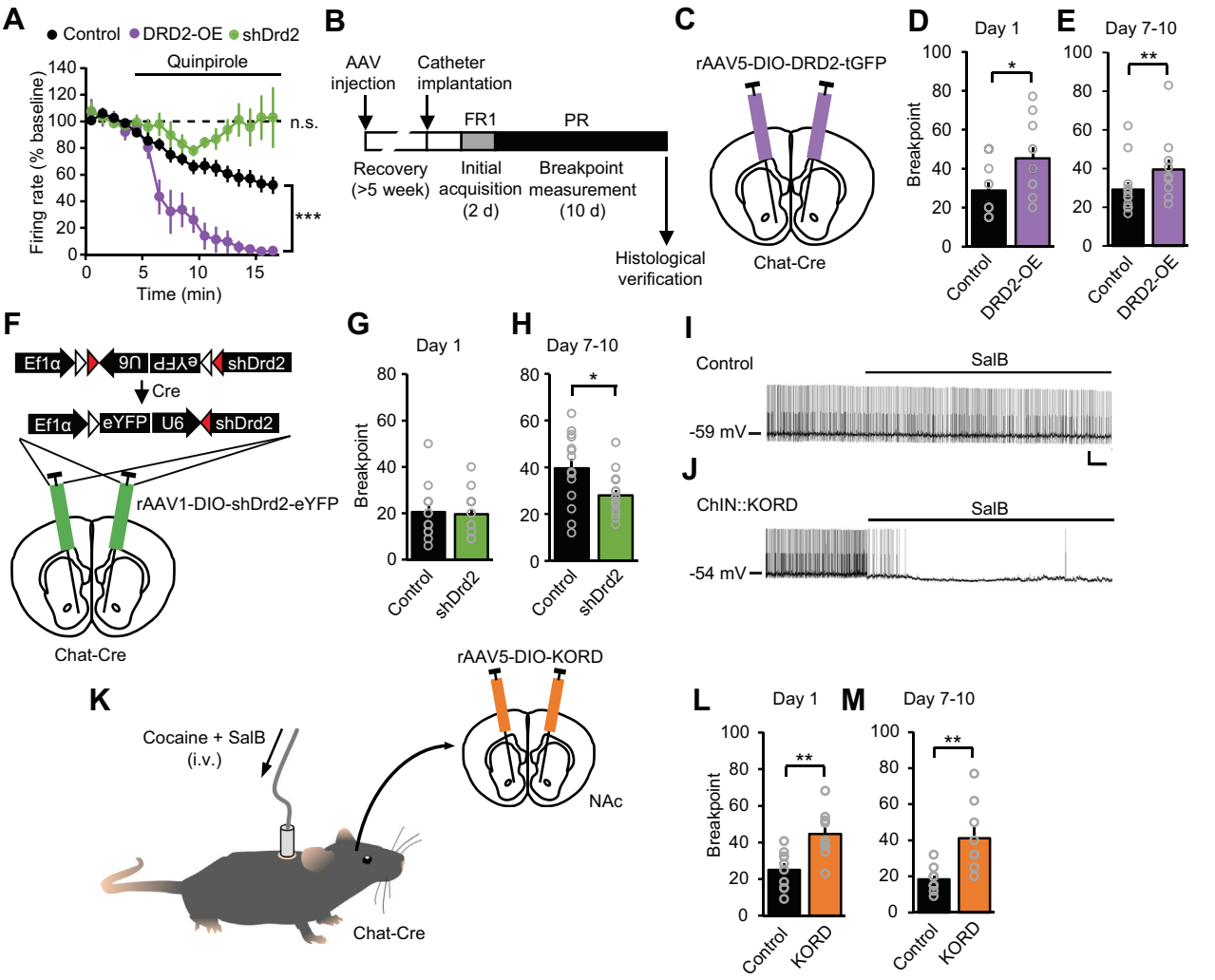

Figure 5. The DRD2 in NAc ChINs is necessary and sufficient for cocaine seeking. **(A)** Electrophysiological verification of DRD2 overexpression and knockdown (shDrd2) (control: $n = 17$ cells; DRD2-OE: $n = 6$ cells; shDrd2: $n = 6$ cells) (1-way repeated-measures analysis of variance for shDrd2 [$F_{17,85} = 0.56$, $p > .1$], 2-way repeated-measures analysis of variance for DRD2-OE vs. control, group × time [$F_{17,85} = 4.99$, $p < .001$]). ***$p < .001$. **(B)** A timeline depicting virus injection and breakpoint measurement. **(C)** Schematic illustration of stereotaxic surgery for AAV-induced overexpression of DRD2 in NAc ChINs. Breakpoints of **(D)** the first day and **(E)** the final 3 days of PR tests after DRD2 overexpression (control: $n = 13$ mice; DRD2-OE: $n = 11$ mice). **(F)** Viral infusion of Cre-dependent shDrd2 into the NAc of Chat-Cre mice. White and red triangles represent lox2722 and TATA-lox, respectively. Breakpoints on **(G)** the first day and **(H)** the final 3 days of PR tests in the Cre-negative control ($n = 14$ mice) and shDrd2 ($n = 16$ mice) groups. Representative whole-cell recording traces from **(I)** an uninfected ChIN and **(J)** designer receptor derived from the KORD-expressing NAc ChIN. Black lines depict bath application of SalB (100 μM). Scale bars = 20 mV and 30 seconds. **(K)** Schematic illustration of breakpoint assessment after bilaterally injecting AAV encoding double-floxed KORD into the NAc of Chat-Cre or Cre-negative control mice. Cocaine and SalB were injected during the PR schedule. Breakpoints on **(L)** the first day and **(M)** the final 7–10 days of PR tests (control: $n = 10$ mice; KORD: $n = 9$ mice). Mann-Whitney U tests were used for comparisons. *$p < .05$, **$p < .01$. Data are presented as mean ± SEM. AAV, adeno-associated virus; Chat, choline acetyltransferase; ChINs, cholinergic interneurons; DIO, double-floxed inverted orientation; DRD2, dopamine D_2 receptor; eYFP, enhanced yellow fluorescent protein; FR, fixed ratio; i.v., intravenous; KORD, kappa opioid receptor; NAc, nucleus accumbens; n.s., not significant; OE, overexpression; PR, progressive ratio; SalB, salvinorin B; tGFP, turbo green fluorescent protein.

abolished quinpirole-induced reduction of spontaneous firing rates in NAc ChINs (Figure 5A and Figure S5E in Supplement 1). Importantly, mice with depleted DRD2 had significantly lower motivation toward cocaine infusion than control animals (Figure 5G, H and Figure S5M, N in Supplement 1). These findings support the notion that DRD2 in NAc ChINs is sufficient and necessary for development and maintenance of susceptibility traits to cocaine addiction.

Inactivation of NAc ChINs Leads to Increased Drug Motivation

DRD2 activation in striatal ChINs induces various physiological changes, including depression of spontaneous neuronal activity, elongation of postburst pause, and disinhibition of Ca^{2+} channels in downstream MSNs (16,30,31). We sought to determine whether the emergence of addiction-like behaviors could result from inhibition of NAc ChIN activity induced by

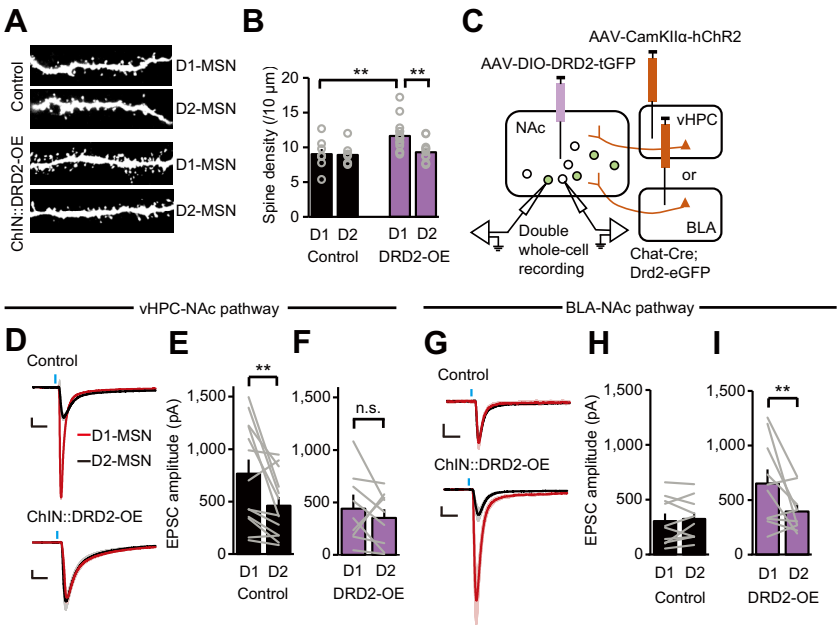

Figure 6. The DRD2 in NAc ChINs is sufficient and necessary to induce cocaine-related cell type– and pathway-specific changes in NAc MSNs. **(A)** Representative images of dendritic spines from D1- and D2-MSNs. A DRD2-encoding AAV was injected into the NAc of Chat-Cre mice (ChIN::DRD2-OE) or Cre-negative mice (control). **(B)** Spine densities from D1- and D2-MSNs of control and DRD2-OE mice (Kruskal-Wallis H test with Dunn's post hoc test for multiple comparison). $^{**}p < .01$, $n \geq 8$ cells for each group. **(C)** Schematic depiction of dual whole-cell recording from D1- and D2-MSNs. ChR2 is expressed in the vHPC or BLA of Chat-Cre × Drd2-eGFP double transgenic mice. **(D)** Example EPSC traces simultaneously recorded from D1-MSNs (red) and D2-MSNs (black) upon stimulation of the vHPC-NAc pathway. Summary of EPSC amplitudes in the vHPC-NAc pathway, recorded in slices from **(E)** Cre-negative control (n = 13 MSN pairs from 5 mice) or **(F)** DRD2-OE (n = 9 MSN pairs from 3 mice) mice. **(G)** Example EPSC traces upon stimulation of the BLA-NAc pathway. Scale bars = 40 ms and 50 pA. Summary of EPSC amplitudes in the BLA-NAc pathway, recorded in slices from **(H)** Cre-negative control (n = 12 MSN pairs from 5 mice) or **(I)** DRD2-OE (n = 9 MSN pairs from 4 mice) mice. Wilcoxon signed rank test was used for analysis of paired recordings. $^{**}p < .01$. AAV, adeno-associated virus; BLA, basolateral amygdala; Chat, choline acetyltransferase; ChINs, cholinergic interneurons; ChR2, channelrhodopsin-2; DIO, double-floxed inverted orientation; DRD2, dopamine D_2 receptor; EPSC, excitatory postsynaptic current; eYFP, enhanced yellow fluorescent protein; i.v., intravenous; MSN, medium spiny neuron; NAc, nucleus accumbens; n.s., not significant; OE, overexpression; tGFP, turbo green fluorescent protein; vHPC, ventral hippocampus.

activation of DRD2. Thus, we inhibited ChIN activity by cell type–specific expression of KORD and its activation by salvinorin B (SalB) administration (19), which is known to exert minimal effects on endogenous DA receptors (33). We expressed KORD selectively in NAc ChINs by using a Cre-dependent AAV vector and Chat-Cre mice, and confirmed that SalB application suppressed spontaneous activity in AAV-infected ChINs but had negligible effect on uninfected control ChINs (Figure 5I, J). Mice expressing KORD in NAc ChINs were intravenously infused with SalB together with cocaine during PR tests (Figure 5K). KORD-expressing mice exhibited higher motivation to cocaine compared with Cre-negative control mice, who also received SalB during cocaine infusion (Figure 5L, M and Figure S5O, P in Supplement 1).

DRD2-Induced Behavioral Changes Are Accompanied by Cell Type–Specific Alteration of Dendritic Spine Density and Excitatory Inputs of MSNs

Chronic cocaine exposure can cause morphological changes in NAc MSNs. Specifically, repeated noncontingent cocaine injection followed by short withdrawal increased dendritic spine density in D1-MSNs but not in D2-MSNs (34). Motivation to cocaine, which was elevated by DRD2 overexpression in ChINs, would be associated with structural changes of neighboring NAc MSNs. Consistent with this notion, D1-MSNs, but not D2-MSNs, exhibited increased spine density after a cell type–specific overexpression of DRD2 in NAc ChINs, despite the absence of cocaine injection (Figure 6A, B).

Chronic exposure to cocaine results in altered excitatory postsynaptic current (EPSC) ratios between D1- and D2-MSNs in a pathway-specific manner (35). After cocaine injection, EPSC ratio of D1-/D2-MSNs increased in the BLA-NAc pathway, but decreased in the vHPC-NAc pathway, while the mPFC-NAc pathway remained unaffected (35). Using ChR2-encoding AAV and Chat-Cre/Drd2-eGFP double transgenic mice, we monitored impacts of ChIN-specific DRD2 overexpression on optically driven EPSCs in distinct MSN subtypes (Figure 6C). In three distinct experiments, ChR2 was expressed in upstream brain regions of the NAc: the vHPC, BLA, or mPFC (Figure 6C and Figure S6A in Supplement 1). Simultaneous whole-cell recording from D1- and D2-MSNs revealed that the EPSC ratio between two MSN subtypes was shifted in a pathway-selective fashion after NAc ChIN-specific DRD2 overexpression in drug-naïve mice. EPSC ratios of D1-/D2-MSNs decreased in the vHPC-NAc pathway (Figure 6D–F) but increased in the BLA-NAc pathway (Figure 6G–I), whereas the mPFC-NAc pathway was unaffected (Figure S6B, C in Supplement 1). To further investigate which component of the EPSCs accounted for DRD2-induced plasticity, we next assessed quantal EPSCs in bath solutions containing Sr^{2+} (Figure S6D in Supplement 1). While both quantal EPSC amplitude and frequency remained unaltered in the mPFC-NAc pathway (Figure S6E, F in Supplement 1), quantal EPSC frequency, but not amplitude, was increased in the BLA-NAc pathway after ChIN-specific DRD2 overexpression (Figure S6G, H in Supplement 1).

We also examined whether DRD2 in NAc ChINs was required for cocaine-induced synaptic alterations in the BLA-NAc and vHPC-NAc pathway, which have been implicated in cocaine craving and sensitization (6,35,36). DRD2 was selectively depleted in NAc ChINs, and ChR2 was expressed in the

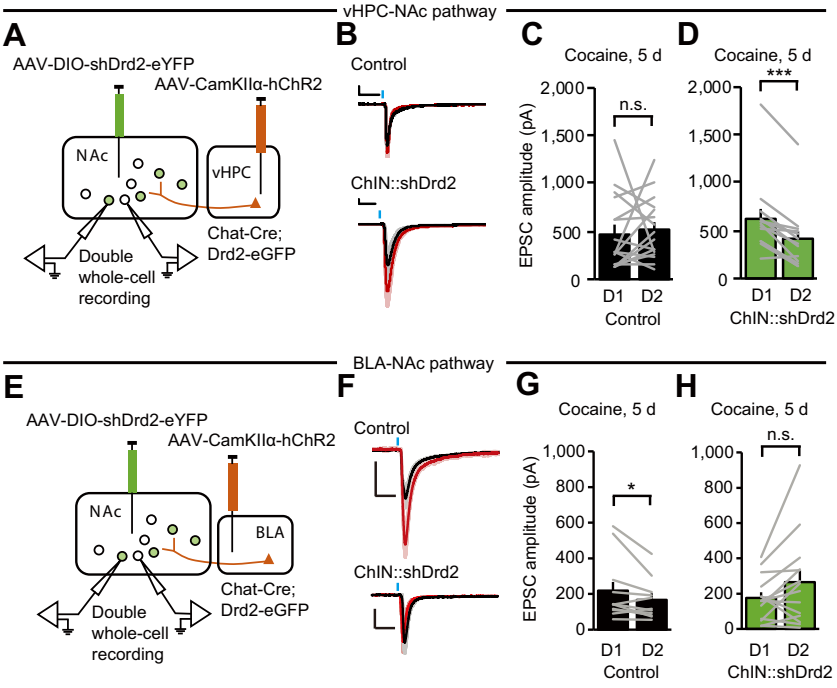

Figure 7. Cre-dependent depletion of ChIN DRD2 in the NAc interferes with cocaine-induced synaptic plasticity in a pathway-specific manner. **(A)** Schematic illustration of the Cre-dependent DRD2 knockdown experiment in the vHPC-NAc pathway. **(B)** Representative EPSC traces induced by optic stimulation of the vHPC-NAc pathway in Cre-negative (control) and DRD2-depleted (ChIN::shDrd2) mice. Recordings were conducted after 1- to 2-day withdrawal from 5-day exposure to cocaine (15 mg/kg, intraperitoneal). **(C, D)** Summary of EPSC amplitudes in D1-MSNs and D2-MSNs of cocaine-injected mice. EPSCs were recorded ex vivo in **(C)** control (n = 11 MSN pairs from 4 mice) or **(D)** ChIN::shDrd2 (n = 14 MSN pairs from 5 mice) mice. **(E)** Schematic illustration for knockdown experiments in the BLA-NAc pathway. **(F)** Representative EPSC traces induced by stimulating the BLA-NAc pathway. **(G, H)** Summary of EPSC amplitudes in D1- and D2-MSNs of **(G)** cocaine-injected control (n = 16 MSN pairs from 5 mice) and **(H)** cocaine-injected ChIN::shDrd2 (n = 13 MSN pairs from 5 mice) mice. Blue bars indicate timing of optic stimulation. Scale bars = 40 ms and 50 pA. Wilcoxon signed rank test was used for analysis of paired-recordings. $^{*}p < .05$, $^{***}p < .001$. AAV, adeno-associated virus; BLA, basolateral amygdala; Chat, choline acetyltransferase; DRD2, dopamine D_2 receptor; ChINs, cholinergic interneurons; DIO, double-floxed inverted orientation; eGFP, enhanced green fluorescent protein; EPSC, excitatory postsynaptic current; eYFP, enhanced yellow fluorescent protein; MSN, medium spiny neuron; NAc, nucleus accumbens; n.s., not significant; vHPC, ventral hippocampus.

vHPC or in the BLA (Figure 7A, E and Figure S7A, B in Supplement 1). Consistent with a previous report (35), the Cre-negative control group showed alteration of EPSC ratios after 5 daily cocaine intraperitoneal injection–attenuated D_1/D_2 EPSC amplitude ratios in the vHPC-NAc pathway but increased D_1/D_2 ratios in the BLA-NAc pathway (Figure 7B, C, F, G). ESPC ratios in both pathways remained unaffected, despite cocaine exposure, when DRD2 was depleted (Figure 7D, H). These data highlight the necessity of DRD2 signaling in ChINs for cocaine-induced synaptic plasticity in both the vHPC-NAc and BLA-NAc pathways. Interestingly, mice harboring DRD2 overexpression in NAc ChINs also displayed elevated locomotion to noncontingent cocaine administration, which was apparent from the first exposure to cocaine (Figure S8A, B in Supplement 1). Collectively, increased abundance of DRD2 induced synaptic plasticity in MSNs and subsequently triggered behavioral sensitization, further substantiating a causal relationship between synaptic plasticity and drug-related behaviors.

DISCUSSION

Here, we demonstrated that DA signaling in NAc ChINs causally controls cocaine-seeking behavior. Our genome-wide analysis of NAc ChINs from susceptible versus resilient animals identified numerous DEGs that could potentially contribute to the emergence of susceptibility traits after cocaine self-administration. Among these DEGs, *Drd2* was upregulated in susceptible animals, and it was sufficient and necessary for development of addiction-like behaviors. We also detected that activation of NAc ChINs during cocaine exposure was blunted in susceptible animals, consistent with the observation that chemogenetic suppression of ChIN activity resulted in elevated drug motivation. This DRD2/ChIN-mediated behavioral change appeared to arise primarily because of pathway-specific synaptic plasticity occurring at MSNs.

By adapting the behavioral paradigm in which rats developed rapid escalation of drug motivation (20), we could segregate susceptible and resilient mice within a relatively short period. The two distinct subpopulations showed a relatively small difference (<15%) of cocaine intake between subpopulations, together with limited lifetime intake (<250 mg/kg). Because exposure to high doses of cocaine could affect release and uptake of DA and consequently alter locomotor responses even after long-term withdrawal (37), identification of susceptible and resilient animals based on volitional seeking with lower cocaine dose may be helpful for investigation of precise mechanisms underlying susceptibility. We further validated that the high-motivation group exhibited core addiction-like behaviors (2). Measurement of each behavioral phenotype in distinct groups could also exclude possibilities of repeated extinction, reinstatement, and association of drug-predicting cues with aversive stimulus, which might affect NAc neuroplasticity (38).

The individual difference of DRD2 abundance is likely to be induced during cocaine self-administration, rather than to arise from innate heterogeneity, not only because we used inbred mice, but also because magnitudes of quinpirole-induced depression of ChIN activity were more widely distributed after completion of the PR schedule. The detailed mechanism by which DRD2 levels are elevated during cocaine

self-administration still remains to be determined. Importantly, DRD2 downstream genes comprising both PKA (protein kinase A)-dependent (*Atf4*, *Creb1*, *Crebbp*, *Prkaca*) and PKA-independent (*Arrb2, Akt1*) signaling pathways were upregulated in NAc ChINs of susceptible mice (Table S2 in Supplement 2) (39). Moreover, our KEGG pathway analysis revealed that signaling pathways previously reported to be altered by exposure to addictive drugs, such as cAMP-PKA-CREB pathways, were also differentially regulated (40). Although cocaine-affected genes previously reported using whole-NAc assessments were conserved in ChINs, by contrast, further comparison with SST+ interneuron data showed only little overlapping of responsive DEGs (Figure S3D in Supplement 1). These results highlight the potential roles of cell type–specific gene regulation between distinct neuronal subtypes for addiction susceptibility.

We established a causal relationship between ChIN activity and motivation to cocaine using multiple genetic tools to control DRD2 abundance specifically in NAc ChINs; DRD2 overexpression in NAc ChINs increased motivation to cocaine and, conversely, DRD2 depletion reduced cocaine-seeking behavior. These results appear to be at odds, considering a previous report suggesting reduced reward-like effect under cocaine-conditioned place preference paired with and optogenetic silencing of ChINs (22). However, it is worth emphasizing that genetic tools that we used, compared with a transient inactivation during single noncontingent cocaine exposure, allow for DRD2 overexpression for at least 5 weeks, which by itself results in MSN synaptic plasticity that could support excessive cocaine seeking (36). Finally, our single-unit recording data indicated that cocaine exposure increased ChIN activity in resilient animals but not in susceptible animals in which the ChIN DRD2 abundance was upregulated. It is reasonable to speculate that ChIN activation during cocaine exposure, which was exhibited by resilient animals, exerts a defensive action and thereby deters the transition to addictive states after cocaine consumption.

Activation of ChINs can increase the release of DA in the NAc by direct activation of nAChRs localized on the axon terminals of DAergic neurons (18). Reduction of ChIN activity is likely to induce susceptibility to cocaine seeking, at least in part through decreased DA release in the NAc, which would occur because of elongated ChIN pausing (17). It was recently shown that the phasic DA release independent of DAergic neuron activity underlies motivation for reward seeking (41), suggesting the physiological significance of locally induced DA release in the NAc. Interestingly, ample evidence indicates that enhanced DA efflux plays a central role in development of reward-like behaviors elicited by cocaine (3), but it was also previously demonstrated that DA levels during cocaine intake diminished after prolonged long-term access to cocaine (42,43). Simultaneous monitoring of ACh and DA concentrations, along with MSN neuronal activity during drug-seeking behavior, will make it possible to delineate their subsecond dynamics, which would be a key regulating factor for synaptic plasticity and addiction-like behaviors. In fact, because both muscarinic ACh receptors and DA receptors are G protein coupled and share downstream signaling pathways, the crosstalk between these two neurotransmitters could yield synergetic or gating effects on signaling molecules critical for synaptic plasticity (44,45).

One of compelling features in this study is that ChIN-specific DRD2 overexpression was sufficient to induce pathway- and cell type–specific synaptic plasticity in MSNs without cocaine exposure. Importantly, all types of synaptic plasticity we observed without cocaine treatment were reminiscent of the alterations observed in mice that received repeated cocaine (34,35). Furthermore, ChIN-specific depletion of DRD2 precluded cocaine-induced alteration of EPSC ratios, indicating a necessary role of ChIN DRD2 for cocaine-induced synaptic plasticity. In the dorsal striatum, DRD2 activity in ChINs was proposed to regulate cell type–specific synaptic plasticity via activation of muscarinic ACh receptors in the corticostriatal pathway (31,45). However, the effects of ChIN DRD2 and presynaptic muscarinic ACh receptors on MSN plasticity have not been fully addressed in the other pathways, especially in the NAc. It is possible that the BLA-NAc and vHPC-NAc circuits can be distinctly regulated by a single signaling pathway, as it has been shown for other types of presynaptic G protein–coupled receptors such as KORDs (46). Furthermore, while it was widely documented that GABAergic (gamma-aminobutyric acidergic) regulation of neuronal activity or spike timing can affect synaptic plasticity (47), effects of ChIN-induced multisynaptic inhibitory transmission (8) on MSN plasticity still remain elusive. Therefore, unraveling the molecular crosstalk and antagonistic interactions among distinct neuronal subtypes and differential cholinergic actions in the NAc will provide new insight into the mechanisms of cocaine addiction.

ACKNOWLEDGMENTS AND DISCLOSURES

This work was supported by the National Research Foundation of Korea Grant Nos. 2017R1A6A3A11035275 (to JHL), 2017M3C7A1048089 (to JWK), 2018M3C7A1024150 (to JWK), 2018R1A3B1052079 (to J-HK), and 2018M3C7A1024152 (to J-HK); Korea Brain Research Institute basic research program Grant Nos. 19-BR-02-05 (to JWK) and 20-BR-04-03 (to JWK); and U.S. National Institute on Drug Abuse Grant Nos. P01DA047233 (to EJN) and R01DA007359 (to EJN).

We thank Dr. M. Poo (Chinese Academy of Science) for constructive discussions and advice throughout the whole study and over this manuscript. We also thank B.S. Kang (SYSOFT, Daegu, Republic of Korea) for analyzing the RNA-sequencing data, and S.J. Jeong (Korea Brain Research Institute) for technical support.

The authors report no biomedical financial interests or potential conflicts of interest.

ARTICLE INFORMATION

From the Department of Life Sciences (JHL, BK, J-HK), Pohang University of Science and Technology, Pohang; Department of Neural Development and Disease (JK, YHJ, JWK), Korea Brain Research Institute, Daegu; Department of Brain and Cognitive Sciences (JK, JWK) and Department of New Biology (JKK), Daegu Gyeongbuk Institute of Science and Technology, Daegu, Republic of Korea; Nash Family Department of Neuroscience (EAR, HK, EJN), Friedman Brain Institute, Icahn School of Medicine at Mount Sinai, New York, New York; and the Department of Psychological and Brain Sciences (PHJ), Krieger School of Arts and Sciences, Johns Hopkins University; and Solomon H. Snyder Department of Neuroscience (PHJ) and Kavli Neuroscience Discovery Institute (PHJ), Johns Hopkins School of Medicine, Johns Hopkins University, Baltimore, Maryland.

EJN, JWK, and J-HK contributed equally to this work.

Address correspondence to Joung-Hun Kim, Ph.D., at joungkim@postech.ac.kr, or Ja Wook Koo, Ph.D., at jawook.koo@kbri.re.kr.

Received Mar 2, 2020; revised Apr 28, 2020; accepted May 5, 2020.

Supplementary material cited in this article is available online at https://doi.org/10.1016/j.biopsych.2020.05.003.

REFERENCES

1. Anthony JC, Warner LA, Kessler RC (1994): Comparative epidemiology of dependence on tobacco, alcohol, controlled substances, and inhalants: Basic findings from the National Comorbidity Survey. Exp Clin Psychopharmacol 2:244–268.
2. Deroche-Gamonet V, David B, Piazza PV (2004): Evidence for addiction-like behavior in the rat. Science 305:1014–1017.
3. Hyman SE, Malenka RC, Nestler EJ (2006): Neural mechanisms of addiction: The role of reward-related learning and memory. Annu Rev Neurosci 29:565–598.
4. Lobo MK, Covington HE 3rd, Chaudhury D, Friedman AK, Sun H, Damez-Werno D, *et al.* (2010): Cell type-specific loss of BDNF signaling mimics optogenetic control of cocaine reward. Science 330:385–390.
5. Kravitz AV, Tye LD, Kreitzer AC (2012): Distinct roles for direct and indirect pathway striatal neurons in reinforcement. Nat Neurosci 15:816–818.
6. Britt JP, Benaliouad F, McDevitt RA, Stuber GD, Wise RA, Bonci A (2012): Synaptic and behavioral profile of multiple glutamatergic inputs to the nucleus accumbens. Neuron 76:790–803.
7. Pascoli V, Terrier J, Espallergues J, Valjent E, O'Connor EC, Lüscher C (2014): Contrasting forms of cocaine-evoked plasticity control components of relapse. Nature 509:459–464.
8. English DF, Ibanez-Sandoval O, Stark E, Tecuapetla F, Buzsáki G, Deisseroth K, *et al.* (2011): GABAergic circuits mediate the reinforcement-related signals of striatal cholinergic interneurons. Nat Neurosci 15:123–130.
9. Gittis AH, Kreitzer AC (2012): Striatal microcircuitry and movement disorders. Trends Neurosci 35:557–564.
10. Atallah HE, McCool AD, Howe MW, Graybiel AM (2014): Neurons in the ventral striatum exhibit cell type–specific representations of outcome during learning. Neuron 82:1145–1156.
11. Gonzales KK, Smith Y (2015): Cholinergic interneurons in the dorsal and ventral striatum: Anatomical and functional considerations in normal and diseased conditions. Ann NY Acad Sci 1349:1–45.
12. Kawaguchi Y, Wilson CJ, Augood SJ, Emson PC (1995): Striatal interneurones: Chemical, physiological and morphological characterization. Trends Neurosci 18:527–535.
13. Berlanga ML, Olsen CM, Chen V, Ikegami A, Herring BE, *et al.* (2003): Cholinergic interneurons of the nucleus accumbens and dorsal striatum are activated by the self-administration of cocaine. Neuroscience 120:1149–1156.
14. Hikida T, Kaneko S, Isobe T, Kitabatake Y, Watanabe D, Pastan I, *et al.* (2001): Increased sensitivity to cocaine by cholinergic cell ablation in nucleus accumbens. Proc Natl Acad Sci U S A 98:13351–13354.
15. Hikida T, Kitabatake Y, Pastan I, Nakanishi S (2003): Acetylcholine enhancement in the nucleus accumbens prevents addictive behaviors of cocaine and morphine. Proc Natl Acad Sci U S A 100:6169–6173.
16. Chuhma N, Mingote S, Moore H, Rayport S (2014): Dopamine neurons control striatal cholinergic neurons via regionally heterogeneous dopamine and glutamate signaling. Neuron 81:901–912.
17. Straub C, Tritsch NX, Hagan NA, Gu C, Sabatini BL (2014): Multiphasic modulation of cholinergic interneurons by nigrostriatal afferents. J Neurosci 34:8557–8569.
18. Threlfell S, Lalic T, Platt NJ, Jennings KA, Deisseroth K, Cragg SJ (2012): Striatal dopamine release is triggered by synchronized activity in cholinergic interneurons. Neuron 75:58–64.
19. Vardy E, Robinson JE, Li C, Olsen RHJ, DiBerto JF, Giguere PM, *et al.* (2015): A new DREADD facilitates the multiplexed chemogenetic interrogation of behavior. Neuron 86:936–946.
20. Morgan D, Liu Y, Roberts DCS (2006): Rapid and persistent sensitization to the reinforcing effects of cocaine. Neuropsychopharmacology 31:121–128.
21. Pascoli V, Terrier J, Hiver A, Lüscher C (2015): Sufficiency of mesolimbic dopamine neuron stimulation for the progression to addiction. Neuron 88:1054–1066.
22. Witten IB, Lin SC, Brodsky M, Prakash R, Diester I, Anikeeva P, *et al.* (2010): Cholinergic interneurons control local circuit activity and cocaine conditioning. Science 330:1677–1681.
23. Robison AJ, Nestler EJ (2011): Transcriptional and epigenetic mechanisms of addiction. Nat Rev Neurosci 12:623–637.
24. Kronman H, Richter F, Labonté B, Chandra R, Zhao S, Hoffman G, *et al.* (2019): Biology and bias in cell type-specific RNAseq of nucleus accumbens medium spiny neurons. Sci Rep 9:8350.
25. Ribeiro EA, Salery M, Scarpa JR, Calipari ES, Hamilton PJ, Ku SM, *et al.* (2018): Transcriptional and physiological adaptations in nucleus accumbens somatostatin interneurons that regulate behavioral responses to cocaine. Nat Commun 9:3149.
26. Lüscher C, Malenka RC (2011): Drug-evoked synaptic plasticity in addiction: From molecular changes to circuit remodeling. Neuron 69:650–663.
27. Vilardaga JP, Jean-Alphonse FG, Gardella TJ (2014): Endosomal generation of cAMP in GPCR signaling. Nat Chem Biol 10:700–706.
28. Lin R, Karpa K, Kabbani N, Goldman-Rakic P, Levenson R (2001): Dopamine D2 and D3 receptors are linked to the actin cytoskeleton via interaction with filamin A. Proc Natl Acad Sci U S A 98:5258–5263.
29. Odagaki Y, Fuxe K (1995): Functional coupling of dopamine D2 and muscarinic cholinergic receptors to their respective G proteins assessed by agonist-induced activation of high-affinity GTPase activity in rat striatal membranes. Biochem Pharmacol 50:325–335.
30. Maurice N, Mercer J, Chan CS, Hernandez-Lopez S, Held J, Tkatch T, *et al.* (2004): D2 dopamine receptor-mediated modulation of voltage-dependent Na^+ channels reduces autonomous activity in striatal cholinergic interneurons. J Neurosci 24:10289–10301.
31. Wang Z, Kai L, Day M, Ronesi J, Yin HH, Ding J, *et al.* (2006): Dopaminergic control of corticostriatal long-term synaptic depression in medium spiny neurons is mediated by cholinergic interneurons. Neuron 50:443–452.
32. Kwon OB, Lee JH, Kim HJ, Lee S, Lee S, Jeong MJ, *et al.* (2015): Dopamine regulation of amygdala inhibitory circuits for expression of learned fear. Neuron 88:378–389.
33. Gomez JL, Bonaventura J, Lesniak W, Mathews WB, Sysa-Shah P, Rodriguez LA, *et al.* (2017): Chemogenetics revealed: DREADD occupancy and activation via converted clozapine. Science 357:503–507.
34. Kim J, Park BH, Lee JH, Park SK, Kim JH (2011): Cell type-specific alterations in the nucleus accumbens by repeated exposures to cocaine. Biol Psychiatry 69:1026–1034.
35. MacAskill AF, Cassel JM, Carter AG (2014): Cocaine exposure reorganizes cell type- and input-specific connectivity in the nucleus accumbens. Nat Neurosci 17:1198–1207.
36. Lee BR, Ma YY, Huang YH, Wang X, Otaka M, Ishikawa M, *et al.* (2013): Maturation of silent synapses in amygdala-accumbens projection contributes to incubation of cocaine craving. Nat Neurosci 16:1644–1651.
37. Mateo Y, Lack CM, Morgan D, Roberts DC, Jones SR (2005): Reduced dopamine terminal function and insensitivity to cocaine following cocaine binge self-administration and deprivation. Neuropsychopharmacology 30:1455–1463.
38. Ebner SR, Larson EB, Hearing MC, Ingebretson AE, Thomas MJ (2018): Extinction and reinstatement of cocaine-seeking in self-administering mice is associated with bidirectional AMPAR-mediated plasticity in the nucleus accumbens shell. Neuroscience 384:340–349.
39. Bonci A, Hopf FW (2005): The dopamine D2 receptor: New surprises from an old friend. Neuron 47:335–338.
40. Levine AA, Guan Z, Barco A, Xu S, Kandel ER, Schwartz JH (2005): CREB-binding protein controls response to cocaine by acetylating histones at the fosB promoter in the mouse striatum. Proc Natl Acad Sci U S A 102:19186–19191.
41. Mohebi A, Pettibone JR, Hamid AA, Wong JT, Vinson LT, Patriarchi T, *et al.* (2019): Dissociable dopamine dynamics for learning and motivation. Nature 570:65–70.

42. Calipari ES, Ferris MJ, Jones SR (2014): Extended access of cocaine self-administration results in tolerance to the dopamine-elevating and locomotor-stimulating effects of cocaine. J Neurochem 128:224–232.
43. Willuhn I, Burgeno LM, Groblewski PA, Phillips PE (2014): Excessive cocaine use results from decreased phasic dopamine signaling in the striatum. Nat Neurosci 17:704–709.
44. Nair AG, Gutierrez-Arenas O, Eriksson O, Vincent P, Hellgren Kotaleski J (2015): Sensing positive versus negative reward signals through adenylyl cyclase-coupled GPCRs in direct and indirect pathway striatal medium spiny neurons. J Neurosci 35:14017–14030.
45. Shen W, Plotkin JL, Francardo V, Ko WK, Xie Z, Li Q, *et al.* (2015): M4 muscarinic receptor signaling ameliorates striatal plasticity deficits in models of L-DOPA-induced dyskinesia. Neuron 88:762–773.
46. Tejeda HA, Wu J, Kornspun AR, Pignatelli M, Kashtelyan V, Krashes MJ, *et al.* (2017): Pathway- and cell-specific kappa-opioid receptor modulation of excitation-inhibition balance differentially gates D1 and D2 accumbens neuron activity. Neuron 93:147–163.
47. Collingridge GL, Isaac JT, Wang YT (2004): Receptor trafficking and synaptic plasticity. Nat Rev Neurosci 5:952–962.